ASTRONOMY & ASTROPHYSICS
SUPPLEMENT SERIES

Astron. Astrophys. Suppl. Ser. **120,** 481-489 (1996)

Models of high-energy emission from active galactic nuclei

R. Schlickeiser

Max-Planck-Institut für Radioastronomie, Postfach 2024, D–53010 Bonn, Germany

Received October 17, 1995; accepted January 31, 1996

Abstract. It is argued that the high-energy X-ray and γ-ray emission from flaring blazars is beamed radiation from the relativistic jet supporting the relativistic beaming hypothesis and the unified scenario for active galactic nuclei (AGNs). Most probably the high-energy emission results from the inverse Compton scattering by relativistic electrons and positrons in the jet of radiation originating *external* to the jet plus intrinsic jet pair annihilation and bremsstrahlung radiation. Direct γ-ray production by energetic hadrons is not important for the flaring phase in γ-ray blazars, but the acceleration of energetic hadrons during the quiescent phase of AGNs may be relevant as the source of secondary electrons and positrons through photo-pair and photo-pion production.

The start of the γ-ray flare is accompanied by the emergence of a new superluminal jet component. Combining time-correlated flux measurements at optical and γ-ray frequencies with contemporaneous VLBI measurements of the apparent transverse speed of the emerging jet component, one finds that a simple diagram relates different classes of radio-loud AGNs and makes definite predictions for the multiwavelength observations of these sources. If an equipartition parameter remains constant between episodes of plasma ejection, then multiple observations of individual sources can in principle determine cosmological parameters

Key words: galaxies: active — gamma-rays: theory — radiation mechanism: non thermal — cosmology: miscellaneous

1. Introduction

Since its launch in April 1991, the experiments on board of the *Compton Gamma Ray Observatory* have detected many extragalactic active galactic nuclei (AGNs) at photon energies > 20 keV:
(1) 51 AGNs have been reported as ($> 5\sigma$) sources (status June 1995) of >100 MeV γ rays (Thompson et al. 1995). Several of them are also seen by the COMPTEL and OSSE instruments (Kurfess 1994). All these AGNs belong to the *blazar category*, i.e. they exhibit high optical polarization, rapid optical variability, flat-spectrum radio emission from a compact core, and very often apparent superluminal ($V_{\rm app} > c$) motion components.
(2) 24 AGNs have been detected by the OSSE experiment in the energy range 50–150 keV (Kurfess 1994): 13 of these are classified as Seyfert 1 galaxies, 5 are Seyfert 2s, 2 are the quasars 3C 273 and 3C 279 and one is the BL-Lac object PKS 2155–304. Five of the sources are also radio galaxies. No Seyfert AGNs or radio galaxies are detected at photon energies above $E_\gamma > 1$ MeV.

Apparently, there exist two classes of γ-ray emitting AGNs (Dermer & Gehrels 1995):
(I) *γ-ray hard blazars* with power law energy spectra extending to energies $\geq$ 10 GeV, and in the case of Mrk 421 (Punch et al. 1992; Macomb et al. 1995; Kerrick et al. 1995) and Mrk 501 (Quinn et al. 1995) even to TeV energies. As I shall argue here, The γ-ray emission in these sources most probably is nonthermal radiation from relativistic jets;
(ii) *γ-ray soft Seyferts* with energy spectra that cut-off sharply above $\sim$ 100 keV. The γ-ray emission from these sources most probably is hot thermal emission from the inner accretion disk (Svensson 1996).

Here I will concentrate on the first class of γ-ray AGNs and discuss the implications of the observations for the nonthermal radiation and particle acceleration processes.

The most remarkable properties of the γ-ray hard blazars are
(1) the high fraction (>15 percent) of superluminal sources (0234+285, 0528+134, 0836+710, 3C 273, 3C 279, 1156+ 295, 1633+382, 2251+158) in the sample;
(2) the dramatic peak of the luminosity spectra (=power per $\lg\nu$) at γ-ray frequencies yielding luminosity ratios much larger unity

$$\rho \equiv \frac{(\nu S_\nu)_\gamma}{(\nu S_\nu)_{\rm radio,mm,optical,X}} >> 1 \qquad (1),$$

which indicates the importance of nonthermal emission processes in these objects;
(3) the short time variability of the γ-ray emission which is observed in most sources (Montigny et al. 1995). Correcting for the redshift z of the sources the intrinsic variability time scale in the cosmological frame $\delta t_i = \delta t_{\rm obs}/(1+z)$ becomes as short as 0.65 days (0528+134), 0.70 days (1633+382), and 1.3 days (3C 279), implying a very compact source from simple light-travel arguments

$$R \leq c\delta t_i \qquad (2);$$

(4) the time-correlated monitoring of the sources at lower frequencies (e.g. Reich et al. 1993; Pohl et al. 1995; Lichti

Send offprint requests to: R. Schlickeiser et al. 1995) which very often demonstrates that the γ-ray flare is accompanied by the optical flare but seems to proceed outbursts at lower frequencies, although exceptions from this rule are frequent.

2. Constraints for AGN models from the γ-ray observations

Because of its rapid variability, its high compactness, lack of radio-quiet sources in the sample and high presence of superluminal motion sources it is generally agreed (Blandford 1993; Dermer 1993; Dermer & Schlickeiser 1992) that the γ-ray emission originates in strongly beamed sources, in accord with the relativistic beaming hypothesis and the unified scenario for AGNs that has served well as the baseline model for the central engines of active galactic nuclei (Blandford & Rees 1978; Scheuer & Readhead 1979; Blandford 1990). Simplifying many details, its basic features read as follows:

(i) AGNs are powered by accretion of matter onto a supermassive black hole;

(ii) in the case of radio-loud AGNs, collimated relativistic jets composed of shocks or plasma blobs move with speed $V_{\rm jet} \sim c$ outward along the axes of the accretion disk. The orientation angle θ^* of the jet axis with respect to the observer in individual AGNs is random;

(iii) the line-of-sight of the observer with respect to the jet axis determines the classification of the particular AGN (for review see Antonucci (1993) and Dermer (1993)).

There are two related powerful arguments that the high-energy X-ray and γ-ray emission is *beamed radiation from the jet*: (1) the absence of intrinsic $\gamma-\gamma$ pair absorption features in the observed γ-ray energy spectra, and (2) the violation of the Elliot-Shapiro relation in at least four γ-ray AGNs. We discuss both in turn.

2.1. Intrinsic compactness

Let us discuss the hypothesis that the high-energy X-ray and γ-ray blazar emission originates as isotropic emission from an uniform spherical (of radius R) source at rest. The optical depth for intrinsic $\gamma + \gamma \to {\rm e}^+ + {\rm e}^-$ attenuation then is (Dermer & Schlickeiser 1994) determined by the source compactness l, i.e. the ratio of the intrinsic source luminosity L to its radius R,

$$\tau \simeq \sigma_{\rm T} n_\gamma R = \frac{\sigma_{\rm T}}{4\pi c < \epsilon >} \frac{L}{R} \quad (3a),$$

where $\sigma_{\rm T}$ denotes the Thomson cross section. Using a mean photon energy $< \epsilon >= 1$ MeV and scaling the intrinsic luminosity in units of the solar luminosity $L_\odot = 2\ 10^{33}$ erg s^{-1} Eq. (3a) becomes

$$\tau = 10^3 \frac{L/L_\odot}{R/{\rm cm}} \quad (3b).$$

The measured γ-ray fluxes above 1 MeV and the known redshifts of the γ-ray blazars imply isotropic intrinsic luminosities of typically $L = 10^{48} L_{48}$ erg s^{-1} (Fichtel et al. 1994) and using the size constraint (2) from the observed time variability in Eq. (3b) yields values of the optical depth

$$\tau \geq 200 \frac{L_{48}}{\delta t_i / 1\ {\rm day}} \quad (3c)$$

much larger than unity. Such large values for the optical depth for pair attenuation are incompatible with the observed straight power law γ-ray energy spectra over four decades of energy, and rule out isotropic emission at rest.

2.2. Violation of the Elliot-Shapiro relation

A second argument against simple isotropic high-energy emission from spherical accretion is given by applying the argument by Elliot & Shapiro (1974) originally developed for X-ray observations. For spherical black hole accretion the source luminosity is limited by the Eddington luminosity

$$L \leq L_{\rm Edd} < 1.3\ 10^{38} \frac{(M/M_\odot)}{\eta}\ {\rm erg\ s^{-1}} \quad (4),$$

where M is the mass of the black hole and $\eta \leq 1$ is a correction factor (Pohl et al. 1995; Dermer & Gehrels 1995) that accounts for the deviation of the Klein-Nishina from the Thomson cross section when calculating the balance between radiation and gravitation forces. Alternatively, the minimum intrinsic time scale for flux variations is

$$\delta t_{i,\rm min} \geq \frac{R_{\rm s}}{c} = 0.98\ 10^{-5} (\frac{M}{M_\odot})\ s \quad (5),$$

since for the generated high-energy photons to escape from the central source the source size has to be larger than the Schwarzschild radius $R_{\rm s}$. Eliminating the mass of the black hole from Eqs. (4) and (5) yields

$$\lg \delta t_{i,\rm min}(s) \geq \lg L({\rm erg\ s^{-1}}) - 43.1 + \lg \eta \quad (6),$$

which for $\eta = 1$ agrees with the Elliot-Shapiro relation. Scaling the observed isotropic unbeamed γ-ray luminosity again as $L = 10^{48} L_{48}$ erg s^{-1} we obtain from Eq. (6) that

$$\lg[\frac{\delta t_{\rm obs}/(1+z)}{\rm days}] \geq \lg L_{48} + \lg \eta \quad (7).$$

In Fig. 1 we compare the observed variability time scales and γ-ray luminosities with the Elliot-Shapiro relation, i.e. Eq. (7) calculated with $\eta = 1$. It can be seen that four sources (0528+134, 1633+382, 3C 279, 1406−076) violate the Elliot-Shapiro relation since they lie in the shaded area below the dividing line. At least for these four sources isotropic emission from a simple steady spherical accreting source at rest is ruled out.

Of course, correcting for deviations from the Thomson cross section, i.e. using a value of $\lg \eta = -1.3$ for a mean photon energy of $< \epsilon >= 10$ MeV, will move the dividing line to the right so that 3C 279 and 1406−076 no longer violate this restriction (as has been pointed out by Pohl et al. (1995) and Dermer & Gehrels (1995)); but on the other hand most of this correction is counterbalanced by the fact that the actual source size is certainly larger than the Schwarzschild radius, say $\sim 10R_s$, so that Eq. (7) with $\eta = 1$ still serves as a good approximation.

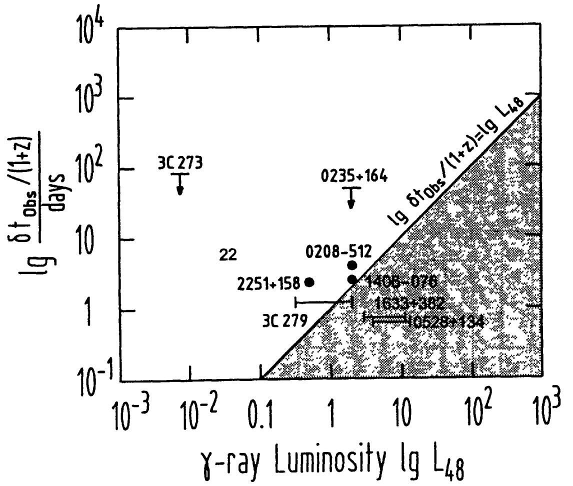

Fig. 1. Comparison of the observed γ-ray variability time scales and luminosities with the Elliot-Shapiro relation for several γ-ray blazars. (From Schlickeiser 1996)

2.3. Relativistic beaming

The discussed absence of photon pair attenuation (Sect. 2.1) and the violation of the Elliot-Shapiro relation (Sect. 2.2) force us to discard the hypothesis of high-energy X-ray and γ-ray emission originating in isotropic sources at rest, and strongly indicate that this emission originates in a source that moves with large bulk speed with respect to us. The natural candidate for this moving source is the relativistic jet hypothesized to exist in AGNs according to the unified scenario. In case of moving sources (with constant speed) the theory of special relativity provides the relation between observed (denoted by an asterisk *) and intrinsic physical quantities (Rybicki & Lightman 1979; Begelman et al. 1984), as

the apparent luminosity $L^*_{\rm app} = \delta^n L, \quad 3 \le n \le 4$ (8a),

the blueshifted frequency $\nu^* = \delta\nu$ (8b),

the Doppler effect upon rate of source variability

$$t^* = t/\delta \qquad (8c),$$

where the Doppler factor

$$\delta = [\Gamma(1-\beta\cos\theta^*)]^{-1}, \quad \beta = V_{\rm jet}/c, \quad \Gamma = (1-\beta^2)^{-1/2} \qquad (8d)$$

is determined by the jet's bulk speed and orientation angle θ^*. The factor n in the Doppler boosting formula (8a) is model dependent, but for many relevant radiation model lies between 3 and 4. A consequence of the Doppler boosting (8a) is that observers are particularly sensitive to AGNs whose jet axis points towards them ($\theta^* \to 0$) since the apparent luminosity from these objects is Doppler boosted by a large factor ($\to (2\Gamma)^n$) compared to intrinsically equally bright AGNs with misaligned jet directions.

Since the *intrinsic* luminosity and source size enter the calculation of the compactness in Eqs. (3) we find with Eqs. (8)

$$l = L/R = \delta^{-(1+n)} \frac{L^*_{\rm app}}{ct^*} \qquad (9)$$

a dramatic reduction by the factor $\delta^{(1+n)}$ in the value of the optical depth (3) to values smaller unity provided $\delta \ge 6$. The same reduction factor applies to the calculation of the Elliot-Shapiro relation and then implies the non-violation of this relation for the four sources 0528+134, 1633+382, 3C 279 and 1406−076. 3C 279 is already a well-known superluminal source and the remaining three are prime candidates for superluminal motion. This prediction of superluminal motion in these sources on the basis of γ-ray observations has been verified by the recent discoveries of superluminal motion components in 0528+134 with apparent speed $\simeq$5c (Pohl et al. 1995) and in 1633+382 with apparent speed $\simeq$6c (Barthel et al. 1995). These discoveries also provide conclusive evidence for a close physical connection between γ-ray flaring and the ejection of new superluminal jet components in blazars (Krichbaum et al. 1995).

2.4. External compactness

In this context the decisive role of external compactness for γ-ray production has to be emphasized. It has been pointed out by many authors (Carraminana 1992; Bednarek 1993a; Blandford 1993; Dermer & Schlickeiser 1994; Sikora et al. 1994; Blandford & Levinson 1995; Becker & Kafatos 1995) that target photon fields external to the jet plasma like the accretion disk photons and/or the reprocessed disk photons in the emission line clouds provide compactness >> 1 inside the γ-ray photosphere. The optical depth for $\gamma-\gamma$ absorption (Dermer & Schlickeiser 1994) produced in the jet at height z above the central black hole due to interactions

– – with accretion disk photons

$$\tau_{\rm A} = 6\ 10^{-6} \frac{L_{46} M_8}{\Theta_{-4} z^2({\rm pc})} \frac{F(E_\gamma)}{F(E_{\gamma,\rm max})} \qquad (10),$$

– – with reprocessed photons

$$\tau_{\rm s} = 0.06 E_\gamma^{0.7}({\rm GeV}) L_{46} \tau_{-2} \ln(z/z_i) \qquad (11),$$

where L_{46} denotes the disk luminosity in units of 10^{46} erg/s, M_8 the black hole mass in units of 10^8 solar masses, τ_{-2} the optical depth for photon scattering in the emission cloud material in units of 0.01, $\Theta_{-4} = 10^4 k_{\rm B} T_{\rm A}/(m_e c^2)$ the dimensionless accretion disk temperature. The height z_i denotes the base of the relativistic jet, $E_{\gamma,\rm max} = 3.6/\Theta_{-4}$ GeV is defined by the maximum value of the function

$$F(x) = \left[x^3[\exp(\frac{2}{\Theta x}) - 1]\right]^{-1} \qquad (12)$$

characterizing the accretion disk's thermal radiation field. The estimate (10) yields γ-ray transparency ($\tau_A < 1$) at heights greater

$$z(\mathrm{pc}) > 2.5 \cdot 10^{-3} L_{46}^{1/2} M_8^{1/2} \Theta_{-4}^{-1/2} \qquad (13),$$

which corresponds to $\simeq 500 M_8^{-1/2} R_s$ Schwarzschild radii. At smaller heights the generated γ-ray photons are severely attenuated. This large size of the γ-ray photosphere is fatal for γ-ray production models close to the central black hole as proposed by Slane & Wagh (1990) and Bednarek (1993b).

The interaction with the reprocessed photons (11) provides transparency ($\tau_s < 1$) at all EGRET energies, in contradiction to Blandford's (1993) conclusion, but would yield strong photon attenuation at TeV energies,

$$\tau_s = 7.5 E_\gamma^{0.7}(\mathrm{TeV}) L_{46} \tau_{-2} \ln(z/z_i) \qquad (14).$$

As a consequence quasars, which have emission line clouds, should not be sources of TeV γ-ray emission. Nearby lineless BL-Lac objects are more likely to be seen at TeV energies.

3. Nonthermal γ-ray emission processes in jets

We now turn our attention to the relevant γ-ray production processes in relativistic jets under the hypothesis that the jets sometimes are filled with blobs containing relativistic charged particles (e^+,e^-,p?) and thermal particles (p,e^-) which are confined to the jet by suitable magnetic fields of strength B_o. The blobs move with relativistic bulk speed V_{jet}, $\Gamma >> 1$. The origin of these jets and blobs are still a matter of intensive debate (e.g. Dermer et al. 1996). Models include MHD winds ejected from the surface of the rotating accretion disk (for review see Blandford 1990; Camenzind 1990), current-free relativistic e^+-e^- beams (Pelletier & Sol 1992), as well as the decay of escaping secondary neutrons produced in inelastic photo-hadron interactions in the central region of the AGN (Contopoulos & Kazanas 1995). It is our hope that the γ-ray observations will provide an important test for these different ideas.

Moreover, we assume that at the start of the γ-ray flare, which is related to the release of a new blob, the relativistic particles in the blob have an initial isotropic power law energy spectrum at height z_i:

$$N(\gamma_i, z_i) = N_o \gamma_i^{-s}, \quad \text{for } \gamma_1 \le \gamma_i \le \gamma_2 \qquad (15).$$

As argued by Schlickeiser (1996) this relativistic particle distribution function may result from "slow" acceleration processes during a "quiescent" AGN phase before the γ-ray flare, and there is no need for rapid particle energization during the γ-ray flare rise time. The total density of relativistic electrons and positrons N_o in Eq. (15) is assumed to be so small that the inverse Compton optical depth

$$\tau_{IC} = \sigma_T N_o r_b = 0.6\left(\frac{N_o}{10^{11}\mathrm{cm}^{-3}}\right)\left(\frac{r_b}{10^{13}\mathrm{cm}}\right) \le 1 \qquad (16)$$

is smaller unity. r_b denotes the size of the blob.

3.1. The role of energetic hadrons

I restrict my discussion here to the emission processes of relativistic electrons and positrons and do not discuss the emission from relativistic hadrons because I am convinced that during the γ-ray flare the latter are less important for the following reasons:

(1) due to their much smaller masses electrons and positrons radiate more efficient than nuclei charge Ze and mass Am_p: for pointlike electromagnetic interactions the "hadron Thomson" cross section

$$\sigma_H = \frac{Z^4}{A^2}\left(\frac{m_e}{m_p}\right)^2 \sigma_T = 1.97\ 10^{-31} \frac{Z^4}{A^2} \quad \mathrm{cm}^2 \qquad (17)$$

is several orders of magnitude smaller than the Thomson cross section;

(2) inelastic hadron (A) interactions such as $A + p \to (\pi^o, \pi^\pm)$, $A + \gamma \to A + e^+ + e^-$, $A + \gamma \to A + (\pi^o, \pi^+, \pi^-)$, $A + \gamma \to (A-1) + N$ (Kazanas & Ellison 1986; Sikora et al. 1987; Mannheim & Biermann 1992; Mastichiadis & Kirk 1995) provide many *secondary* electrons and positrons, and, although hadrons serve as source, the observed radiation is generated in interactions of these secondary electrons and positrons;

(3) the photopair, pion and photopion production processes mentioned under (2) operate most efficiently in regions of high target photon and matter densities, i.e. close to the central black hole. But as shown in Sect. 2.4 such a thick target will be optically thick for the generated γ-rays, and therefore not in accord with the observed straight power law γ-ray energy spectra and the short variability.

To summarize: hadron acceleration may be important during the quiet phase of γ-ray AGNs as source of secondary electrons and positrons, but during the flaring phase the γ-ray radiation is produced by electrons and positrons probably of secondary origin.

3.2. Nonthermal γ-ray production by relativistic electrons and positrons

There are four main radiation production processes by relativistic electrons and positrons that are important in relativistic jets:

(1) *the synchrotron-self Compton (SSC) process*: the relativistic electrons and positrons in the jet inverse Compton scatter their own synchrotron radiation to γ-ray energies (Bloom & Marscher 1993; Maraschi et al. 1993);

(2) *inverse Compton scattering of radiation external to the jet*: the relativistic electrons and positrons in the jet inverse Compton scatter

– the accretion disk photons (Dermer et al. 1992; Dermer & Schlickeiser 1993). The anisotropy of the incoming target photons in combination with the angular dependence of the relativistic Doppler boosting favours γ-ray emission at observer's angles where the source exhibits superluminal motion. This γ-ray production process succesfully explains the key observational features as (i) the peak of the bolometric luminosity at γ-ray frequencies (ii) the γ-ray variability time scale $\leq$ few days, (iii) the softening of the spectra between the hard X-ray and medium γ-ray regime, (iv) the high percentage of superluminal sources in the sample, (v) the generation of TeV emission for favourably aligned observers;

– the accretion disk photons reflected from the material through which the jet is passing as e.g. the emission line clouds in quasars (Sikora et al. 1994);

– photons from the universal 2.7 K microwave background and optical photons from the central star cluster;

(3) *pair annihilation radiation*: the relativistic electrons and positrons in the jet annihilate and including all spectral broadening effects due to the energy distribution of the annihilating particles and the jet bulk motion give rise to broad continuum emission in the MeV γ-ray energy range (Henri et al. 1993; Böttcher & Schlickeiser 1996). If the blobs in the jet also contain thermal electrons the relativistic positrons additionally can annihilate with the thermal electrons;

(4) *pair bremsstrahlung radiation*: the relativistic electron and positron pairs in the jet generate nonthermal bremsstrahlung radiation. Including again all spectral broadening effects due to the energy distribution of the pairs and the jet bulk motion Böttcher & Schlickeiser (1995) have demonstrated that the bremsstrahlung emission from a purely leptonic jet dominates the pair annihilation radiation provided the pair's power law energy distribution functions in the jet have lower energy cutoffs at Lorentz factors $\gamma_1 \gtrsim 5$ and are relatively flat (spectral index $s \lesssim 2.3$). The universal shape of the pair bremsstrahlung hard X-ray spectrum (below intrinsic photon energies $h\nu \leq \gamma_1 \mathrm{mc}^2$) with $\nu S_\nu \propto \nu^{0.9}$ seems to be in good agreement with the hard X-ray spectra observed in many blazars. At large photon energies ($h\nu \geq \gamma_1 \mathrm{mc}^2$) the bremsstrahlung spectrum follows the particle energy distribution function $\nu S_\nu \propto \nu^{2-s}$, thus offering a plausible explanation for strong spectral breaks $\Delta\alpha = s - 1.1$ at several MeV reported for a few objects (McNaron-Brown et al. 1995).

3.3. Comparison of leptonic γ-ray production processes

While the γ-ray yield from production processes (3) and (4) scales with the product of positron and electron pair densities $N_0^+ N_0^-$, the yield from inverse Compton processes (1) and (2) scales with the total pair density times the respective number density of target photons $(N_0^+ + N_0^-) n_{\mathrm{ph}}$. For typical AGN jet parameters one (see Böttcher & Schlickeiser 1996) infers that at pair densities less than $N_c \simeq 10^{10}$ cm^{-3} the inverse Compton processes dominates the γ-ray production in these objects, while at higher pair densities the annihilation and bremsstrahlung radiation take over.

To discriminate any further between the different inverse Compton models is more complex. The observed EGRET γ-ray energy spectra alone are inconclusive to decide on the issue of the most important γ-ray production process in blazars. Advocates of the individual processes have produced remarkable good fits to the EGRET observations. The best tests for the proposed models will be provided by multifrequency time-correlated monitoring of these sources that now are operating (e.g. Lichti et al. 1995).

In any case it is important to realize that probably all four basic radiation mechanisms contribute to the observed γ-ray emission during different phases of the flare with individual contributions that vary as a function of time or height z of the blob above the central object. Moreover, each of these four γ-ray production processes has different Doppler boosting factors and antenna characteristics so the estimate of the relative importance depends strongly on the observer's viewing angle. Another complicating factor is the shortness of energy loss times of the radiating particles implying that the time evolution of the energy spectra of the relativistic electrons and positrons has to be taken into account; not all theoretical calculations include this crucial issue. Within all these caveats on the basis of estimates for the total electron loss rates in the various interaction processes (see Dermer & Schlickeiser 1993, 1994 for details), we find that for parameters appropriate to 3C 279, the inverse Compton scattering of accretion disk photons dominates the production of γ-rays by

– microwave scattering if

$$z(\mathrm{pc}) < 360 \frac{L_{46}^{1/2}}{(\Gamma/10)^2(1+z)^2},$$

– Compton scattering of stellar optical photons if

$$z(\mathrm{pc}) < 4.3\, \frac{(L_\mathrm{d}/L_\mathrm{opt})^{1/2}}{(\Gamma/10)},$$

– the synchrotron-self Compton process if

$$z(\mathrm{pc}) < 0.1\, \frac{L_{46}^{1/2}}{\Gamma(B_\mathrm{o}/1\ \mathrm{G})},$$

– Comptonization of scattered radiation if

$$z(\mathrm{pc}) < 0.06\, \frac{M_8^{1/3} R_{\mathrm{LC}}^{2/3}(\mathrm{pc})}{\tau_{-2}^{1/3}},$$

where M_8 denotes the central black hole mass in units of 10^8 solar masses, R_{ELC} the distance in units of pc of the emission line clouds from the central black hole, and τ_{-2} the electron scattering optical depth in emission line clouds in units of 10^{-2}. Note that the lack of an observed soft X-ray turnover due to photoelectric absorption in contemporaneous GINGA observations of 3C 279 constrains the value $\tau_{-2} \leq 0.25$.

The above constraints together with the size estimate (13) for the γ-ray photosphere place the location of the γ-ray emission site at distances beyond $z \geq 10^{15}$ cm from the central object, which is comparable to the radial extent of the accretion disk and is determined by the obvious absence of $\gamma - \gamma$ pair attenuation in the observed γ-ray spectra.

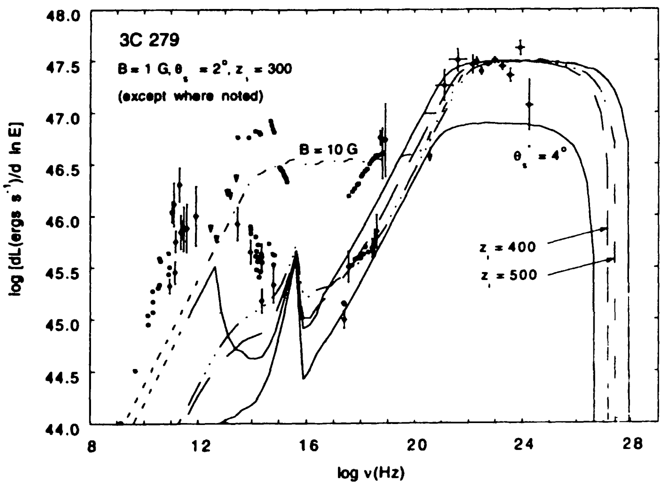

Fig. 2. Model results for the time-integrated luminosity spectrum compared to the multiwavelength observations of 3C 279. The radio-through-optical synchrotron emission, which is probably made farther out in the radio jet, is not modelled here. z_i denotes the starting height of the blob at the beginning of the flare in units of half of the Schwarzschild radius of the central object. From Dermer & Schlickeiser (1993)

γ-ray production by inverse Compton scattering of accretion disk photons by outflowing relativistic electrons and positrons in a relativistic jet is a very economical process: for favorable viewing conditions of the observer a total energy in relativistic electrons and positrons in the blob of

$$E_{\rm tot} \geq 10^{52} (r_{\rm b}/10^{16}\ {\rm cm})^2 (\gamma_1/10)\ {\rm erg} \qquad (18)$$

is sufficient to explain the observed intensities. The estimate (18) results from the source variability constraint (see Eqs. (2) and (8c)) $r_{\rm b} \leq \delta c t^* = 2.6\ 10^{15} \delta (t^*/1\ {\rm day})$ cm, and the requirement (16) of an inverse Compton optical depth smaller unity. Combined with the observed γ-ray luminosity $L(> 100\ {\rm MeV}) = 10^{48} L_{48} f$ erg s^{-1}, where f is the beaming factor, Eq.(18) implies that the intrinsic relativistic electron and positron loss time

$$t_{\rm R} = E_{\rm tot}/L(> 100\ {\rm MeV}) \geq$$

$$10^6 L_{48}^{-1} (f/10^{-2})^{-1} (r_{\rm b}/10^{16}\ {\rm cm})^2 (\gamma_1/10)\ {\rm sec} \qquad (19).$$

Coupled with the Doppler time-dilation effect (Eq. (8c)), we see from Eq. (19) that very short γ-ray flare durations on the order of a few days can easily be explained in this model. However, the short radiation loss time (19) implies that the time evolution of the electron energy spectrum during the γ-ray flare has to be taken into account consistently.

Dermer & Schlickeiser (1993) calculated the time-integrated γ-ray emission from a modified Kardashev-model by instantaneously injecting the power law electron distribution (15) at height z_i at the beginning of the flare, calculating its modification with height in the relativistically outflowing blob due to the operation of the various inverse Compton energy loss processes, and finally integrating the hard X-ray and γ-ray emissivities over height. Comparison with multiwavelength observations of 3C 279 is shown in Fig. 2. One notices the good fit to the time-integrated high-energy emission from this source, including the break by $\Delta\alpha = 0.5$ at MeV energies which results from incomplete relativistic electron cooling. Moreover the peak of the luminosity spectrum at γ-ray energies is well reproduced by the model.

Recently Dermer et al. (1997) have extended the calculation of the evolution of the radiating electron distribution function by including additional Coulomb and bremsstrahlung losses with a cold jet component. This extension gives rise to spectral breaks by $\Delta\alpha = 1.0$ at MeV energies in the time-integrated γ-ray spectrum.

3.4. Luminosity peak

The dramatic peak of the luminosity spectra at γ-ray frequencies with values of ρ (see Eq. (1)) exceeding 10 in many flaring blazars (with the exception of 3C 273 and some BL Lac objects) is a key observational result that strongly favours the external Compton scattering model over the SSC model. In the former this is most naturally explained by the different Doppler factor dependence of the synchrotron and external inverse Compton flux: as shown by Dermer et al. (1997) (see also Dermer 1995) the ratio of the νF_ν spectral power in the synchrotron and Compton components is given by

$$\rho \simeq k \delta^{1+\alpha} \qquad (20),$$

where $k = u_{\rm iso}/u_{\rm B}$ denotes the ratio of the energy densities in the external target radiation field and the blob's magnetic field, while $\alpha \gtrsim 1$ is the measured energy spectral index of the Compton scattered photon power law flux. As Eq. (20) indicates, values of $\rho \geq 10$ quite naturally arise provided the equipartition parameter k is of order unity in these objects. The relation (20) states that the γ-ray radiation is more beamed than the synchrotron emission which nicely accounts for the observational fact that radio galaxies are not EGRET sources which according to the unification scenario for radio-emitting AGNs (e.g., Woltjer 1990) are observed at large viewing angles with respect to the axis of a jet of relativistically outflowing plasma.

At least in simple single homogeneous SSC models it is difficult to understand values of ρ larger than unity since here the Doppler factor dependence of the synchrotron and inverse Compton components is the same. Interpreting the

γ-ray emission as the first SSC component the luminosity ratio is determined solely by intrinsic source parameters (see Dermer et al. 1997)

$$\rho_{\rm SCC} \simeq \tau_{\rm IC}(\epsilon_{\rm C}/\epsilon_{\rm S})^{1-\alpha} \quad (21),$$

where the ratio of the Compton scattered photon energy ($\epsilon_{\rm C}$) to the synchrotron photon energy ($\epsilon_{\rm S}$) is a large quantity $\epsilon_{\rm C}/\epsilon_{\rm S} \simeq \gamma^2 >> 1$. As a consequence, Eq. (21) yields values much less than unity, since $\alpha \geq 1$ and $\tau_{\rm IC} < 1$ according to Eq. (16), in obvious conflict with the observations.

4. Prospects of correlated multiwavelength campaigns

If external inverse Compton scattering in relativistic jets indeed is the relevant γ-ray production process the combination of correlated measurements of the inverse Compton component (at γ-ray frequencies) and the synchrotron component (at mm, infrared and/or optical frequencies) during the γ-ray flare yields according to Eq. (20) an independent determination of the Doppler factor δ of the emerging jet component. As pointed out by Schlickeiser and Dermer (1995) we can simply invert Eq. (20) to obtain δ in terms of the measured values of ρ and α, giving

$$\delta = (\frac{\rho}{k})^{1/(1+\alpha)} \equiv \chi. \quad (22)$$

The relation between the measured apparent superluminal transverse speed βc, the blob's speed Bc, and the observing angle θ^* is given by

$$\beta = \frac{B\sqrt{1-\mu^2}}{1-B\mu} \quad (23),$$

where $\mu = \cos\theta^*$ (see Rees 1966; Rybicki & Lightman 1979). Equations (8d), (22) and (23) can be combined into the expression[1]

$$\theta^* = \arctan[\frac{2\beta}{\chi^2+\beta^2-1}]. \quad (24)$$

In Fig. 3 we show the relationship between β and the Compton/synchrotron parameter χ for different values of θ^* and the bulk Lorentz factor Γ. By following lines of constant Γ, we see that as δ or χ increases, β rises from 0 at large values of θ^* to its maximum value ($= B\Gamma$) at the observing angle $\theta^*_{\rm SL} = \cos^{-1} B$, returning to small values at small observing angles. For a value $\Gamma = 10$, which may be typical of quasars, moderate values of β between 0 and 5 occur when viewing at large angles $\theta \gtrsim 15°$ to the jet axis. This is when δ or χ is small, so we expect a small ratio of γ-ray power to synchrotron power. At shallow angles $\theta \simeq 3°-10°$, superluminal speeds $\beta \approx B\Gamma$ will be observed, corresponding to moderate or large values of χ. For the rare cases where we are viewing a few degrees or less to the jet axis, large values of χ should accompany small values of β.

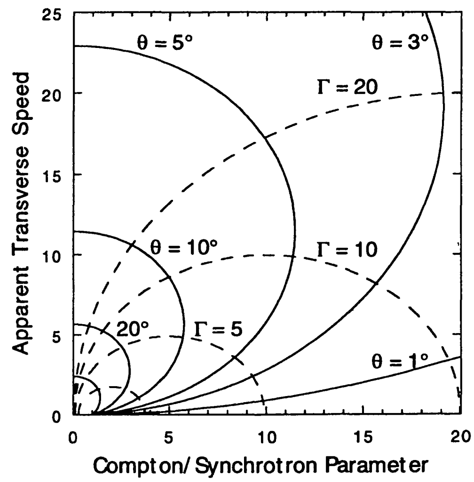

Fig. 3. Relation between apparent transverse speed β and the Compton/synchrotron parameter χ for different values of the observing angle θ^* with respect to the jet direction (solid curves) and the bulk Lorentz factor Γ (dashed curves). The innermost solid curve is calculated for $\theta^* = 45°$ and the innermost dashed curve for $\Gamma = 2$

Supermassive black holes should have considerable gyroscopic stability and would therefore eject plasma along fairly well-defined axes. We can thus chart the expected relation between β and χ for a given source. This is given by curves of constant θ^* in Fig. 3, where we see that a single source ejecting plasma along a fixed axis but with variable values of Γ would display values of β and χ that follow a prescribed trajectory for a fixed value of the equipartition value k.

A definite test of these kinematic relations based upon an external Compton-scattering model for the γ-rays will require correlated VLBI, mm-through-optical monitoring of the synchrotron component, and γ-ray monitoring of the Compton component. At present, there are only a few correlated multiwavelength campaigns which monitor both the synchrotron emission above strongly self-absorbed frequencies ($\gg$100 GHz) and the Compton component at γ-ray energies, including 3C 273 (Lichti et al. 1995), 3C 279 (Maraschi et al. 1994), PKS 0528+134 (Pohl et al. 1995), and Mrk 421 (Macomb et al. 1995). For PKS 0528+134 (Krichbaum et al. 1995) and 3C 279 (Wehrle et al. 1994), correlated VLBI studies have been performed, but final results are not yet available.

4.1. Determination of source parameters and the Hubble constant

Of particular interest are γ-ray blazars that undergo several outbursts. Lately it has been established for the blazars 0534+134 (Pohl et al. 1995; Krichbaum et al. 1995), 3C 279 (Wehrle et al. 1994), 3C 454.3 (Krichbaum

[1] Note that Eqs. (5)-(7) in Schlickeiser & Dermer (1995) are incorrect: in Eq. (5) it has to be χ^2 instead of χ in the argument of the arctan-function.

et al. 1995) and 1633+382 (Barthel et al. 1995) that enhanced levels of activity in the optical and γ-ray bands are associated with the emergence of new jet components. Assuming that the observing angle θ^*, the equipartition parameter k and the energy spectral index α entering Eq. (22) remain constant at different blob ejections, then observations of two different blobs can uniquely determine the values of θ^* and the equipartition parameter k. For blazars with two emerging outbursts and measured values of (β_1, ρ_1) and (β_2, ρ_2), we infer that the equipartition parameter has the value (correcting again for the error in Eq. (6) of Schlickeiser & Dermer (1995) - see footnote 1)

$$k = \left[\frac{\beta_1 \rho_2^{2/(1+\alpha)} - \beta_2 \rho_1^{2/(1+\alpha)}}{(\beta_1 - \beta_2)(1 + \beta_1 \beta_2)}\right]^{\frac{1+\alpha}{2}} \qquad (25),$$

while the observing angle θ^* follows from Eq. (24) after inserting Eqs. (22) and (25).

It has been emphasized by Schlickeiser & Dermer (1995) that the determination of the apparent speed β depends on the Hubble constant $H_0 = 75\text{h km s}^{-1}\text{ Mpc}^{-1}$ (e.g. Pearson & Zensus 1987) through the relation

$$\beta = \frac{126}{h}[1 - \frac{1}{\sqrt{1+z}}](\frac{T}{\text{mas/yr}}), \qquad (26)$$

given the measurered proper motion T for a $\Omega = 1$, $\Lambda = 0$ universe. Under the same assumptions given above, the observation of a third ejection can determine the value of the Hubble constant h. This discussion indicates the very high potential of the ongoing contemporaneous multiwavelength campaigns if combined with VLBI observations of these sources not only for the determination of intrinsic source parameters (as the observing angle θ^* and the equipartition parameter k) but also for cosmological parameters.

5. Summary and conclusions

In this work I have argued that the high-energy X-ray and γ-ray emission from flaring blazars is beamed radiation from the relativistic jet supporting the relativistic beaming hypothesis and the unified scenario for AGNs. Most probably the high-energy emission results from inverse Compton scattering by relativistic electrons and positrons in the jet of radiation originating *external* to the jet plus pair annihilation and bremsstrahlung radiation from the jet. Future positive TeV detections of EGRET AGN sources will be decisive to identify the prominent target photon radiation field. The model of Sikora et al. (1994), where reprocessed accretion disk photons in the emission line region are comptonized, apparently does not operate in lineless BL Lac objects and implies significant intrinsic $\gamma - \gamma$ pair attenuation of the generated TeV photons. In the model of Dermer & Schlickeiser (1993), where the accretion disk photons are comptonized, TeV emission is possible from nearby BL Lac objects but triplet pair production and the extreme Klein-Nishina cutoff will give rise to a significant steepening of the γ-ray energy spectra in this range, whereas in quasars the intrinsic $\gamma - \gamma$ attenuation from the reprocessed radiation absorbs the TeV photons. The synchrotron-self Compton models are extremely inefficient at TeV energies due to the extreme Klein-Nishina limit of the second Compton upscattering of MeV photons, and in quasars also suffer from the $\gamma - \gamma$ attenuation. Direct γ-ray production by energetic hadrons is not important for the flaring phase in γ-ray blazars, but the acceleration of energetic hadrons during the quiescent phase of AGNs may be relevant as the source of secondary electrons and positrons through photo-pair and photo-pion production.

If the γ rays from radio-loud active galactic nuclei are generated by relativistic electrons in the jet which Compton scatter radiation from outside the jet, such as the direct or rescattered accretion-disk photons, then the ratio of the power in the high-energy Compton component to the power in the low-energy synchrotron component is simply related by Eq. (20), which depends on the observing angle to the jet and the plasma outflow speed. This implies that the γ rays are emitted into a narrower cone than the synchrotron radiation. The combination of this relation with contemporaneous VLBI measurements of apparent transverse speed leads to a simple diagram that relates different classes of radio-loud active galactic nuclei (AGNs) and makes definite predictions for multiwavelength observations of these sources. Observations of a single source at different episodes of plasma ejection can determine intrinsic source parameters and, in principle, measure the Hubble constant.

Acknowledgements. I am grateful to my main collaborators C.D. Dermer, M. Böttcher, H. Mause, W. Reich and M. Pohl for their cooperation, support and encouragement. I thank the DARA (50 OR 94063) for partial support of my Compton observatory guest investigator programs.

References

Antonucci R., 1993, ARA&A 31, 473
Barthel P.D., et al., 1995, ApJ 444, L21
Becker P.A., Kafatos M. 1995, ApJ 453, 83
Bednarek W., 1993a, A&A 278, 307
Bednarek W., 1993b, ApJ 402, L29
Begelman M.C., Blandford R.D., Rees M.J., 1984, Rev. Mod. Phys. 56, 255
Blandford R.D., 1990, in Active Galactic Nuclei, T. Courvoisier & M.Mayor (eds.). Springer, Berlin, p. 161
Blandford R.D., 1993, in Compton Gamma-Ray Observatory, M. Friedlander, N.Gehrels & D.J. Macomb (eds.). AIP, New York, p. 533
Blandford R.D., Rees M.J., 1978, in Pittsburgh Conf. on BL Lac Objects, A.M. Wolfe (ed.). Pittsburgh University Press, Pittsburgh, p. 328
Blandford R.D., Levinson A., 1995, ApJ 441, 79
Bloom S.D., Marscher A.P., 1993, Proceedings of the Compton Symp., N. Gehrels & M. Friedlander (eds.). New York, AIP, p. 578
Böttcher M., Schlickeiser R., 1995, A&A 302, L17

Böttcher M., Schlickeiser R., 1996, A&A 306, 86
Camenzind M., 1990, Rev. Mod. Astron. 3, 234
Carraminana A., 1992, A&A 264, 127
Contopoulos J., Kazanas D., 1995, ApJ 441, 521
Dermer C.D., 1993, Proceedings of the Compton Symp., N. Gehrels & M. Friedlander (eds.). New York, AIP, p. 541
Dermer C.D., 1995, ApJ 446, L63
Dermer C.D., Gehrels N., 1995, ApJ 447, 103
Dermer C.D., Miller J.A., Li H., 1996, ApJ 456, 106
Dermer C.D., Schlickeiser R., 1992, Sci 257, 1642
Dermer C.D., Schlickeiser R., 1993, ApJ 416, 458
Dermer C.D., Schlickeiser R., 1994, ApJS 90, 945
Dermer C.D., Schlickeiser R., Mastichiadis A., 1992, A&A 256, L27
Dermer C.D., Sturner S.J., Schlickeiser R., 1997, ApJS 109 (in press)
Elliot J.D., Shapiro S.L., 1974, ApJ 192, L3
Fichtel C.E., et al., 1994, ApJS 94, 551
Henri G., Pelletier G., Roland J., 1993, ApJ 404, L41
Kazanas D., Ellison D., 1986, ApJ 304, 178
Kerrick A.D., et al., 1995, ApJ 438, L59
Krichbaum T.P., et al., 1995, in Quasars and AGN, M. Cohen & K. Kellerman (eds.), Proc. Nat. Acad. Sci. 92, 11377
Kurfess J.D., 1994, in Active Galactic Nuclei Across the Electromagnetic Spectrum, IAU Symp. 159, T. Courvoisier & A. Blecha (eds.). Dordrecht, Kluwer, p. 39
Lichti G.G., et al., 1995, A&A 298, 711
Macomb D.J., et al., 1995, ApJ 449, L99
Mannheim K., Biermann P.L., 1992, A&A 253, L21
Maraschi L., Ghisellini G., Celotti A., 1993, ApJ 397, L5
Maraschi L., et al., 1994, ApJ 435, L91
Mastichiadis A., Kirk J.G., 1995, A&A 295, 613
McNaron-Brown K., et al., 1995, ApJ 451, 575
Montigny C. von, et al., 1995, ApJ 440, 525
Pearson T.J., Zensus J.A., 1987, in Superluminal Radio Sources, J.A. Zensus & T.J. Pearson (eds.). Cambridge Univ. Press, New York, p. 1
Pelletier G., Sol H., 1992, MNRAS 254, 635
Pohl M., et al., 1995, A&A 303, 383
Punch M., et al., 1992, Nat 358, 477
Quinn J., et al., 1995, IAU Circ. No. 6178
Rees M.J., 1966, Nat 211, 468
Reich W., et al., 1993, A&A 273, 65
Rybicki G.B., Lightman A.P., 1979, Radiative Processes in Astrophysics. John Wiley, New York
Scheuer P.A.G., Readhead A.C.S., 1979, Nat 277, 182
Schlickeiser R., 1996, Space Sci. Rev. 75, 299
Schlickeiser R., Dermer C.D., 1995, A&A 300, L29
Sikora M., Begelman M.C., Rees M.J., 1994, ApJ 421, 153
Sikora M., Kirk J.G., Begelman M.C., Schneider, P., 1987, ApJ 320, L81
Slane P., Wagh S.M., 1990, ApJ 364, 198
Svensson R., 1996, (this conference)
Thompson D.J., et al., 1995, ApJS 101, 259
Wehrle A.E., et al., 1994, in The Multimission Perspective, Eureka Scientific, Napa Valley, p. 27
Woltjer L., 1990, in Active Galactic Nuclei, T. Courvoisier & M.Mayor (eds.). Springer, Berlin, p. 7